Volume 37
Number 13
June 29, 1998

Inorganic Chemistry



# Articles

## Synthesis, Structure, and Characterization of the New $[L(OH)Fe(\mu\text{-}O)Fe(OH_2)L]^{3+}$ Complex (L = *N*,*N*′-Dimethyl-*N*,*N*′-bis(2-pyridylmethyl)ethane-1,2-diamine). Detection of an Equilibrium with the Protonated Diamond Form $[LFe(\mu\text{-}O)(\mu\text{-}OH)FeL]^{3+}$ in Acetonitrile

**Sandrine Poussereau,[†] Geneviève Blondin,*[,†] Michèle Cesario,[‡] Jean Guilhem,[‡] Geneviève Chottard,[§] Florence Gonnet,[||] and Jean-Jacques Girerd[†]**

Laboratoire de Chimie Inorganique, URA CNRS 420, Institut de Chimie Moléculaire d'Orsay, Université Paris-Sud, 91405 Orsay Cedex, France, Institut de Chimie des Substances Naturelles, UPR CNRS 2301, 91198 Gif-sur-Yvette, France, and Laboratoire de Chimie des Métaux de Transition, URA CNRS 419, and Laboratoire de Chimie Structurale Organique et Biologique, UMR CNRS 7613, Université Pierre et Marie Curie, 75252 Paris Cedex 05, France

*Received December 19, 1997*

The complex $[L(H_2O)Fe(\mu\text{-}O)Fe(OH)L](ClO_4)_3 \cdot H_2O$, where L = *N*,*N*′-dimethyl-*N*,*N*′-bis(2-pyridylmethyl)ethane-1,2-diamine, was synthesized. It crystallizes in the orthorhombic space group $P2_12_12_1$ with $a = 13.283(5)$ Å, $b = 16.050(9)$ Å, $c = 20.050(9)$ Å, $V = 4476(6)$ Å$^3$, and $Z = 4$. It presents the hydrogen-bonded $[(H_2O)Fe(\mu\text{-}O)Fe(OH)]^{3+}$ core unit characterized by an Fe−O−Fe angle of 137.5(2)° and an Fe−Fe distance of 3.396(1) Å. The measurement of the magnetic susceptibility as a function of the temperature indicated an antiferromagnetic coupling between the two high-spin Fe(III) ions $J = -184$ cm$^{-1}$ ($H = -J\mathbf{S_1}\cdot\mathbf{S_2}$). In the solid state the symmetric stretching vibration was observed at 438 cm$^{-1}$. Upon dissolution in dry acetonitrile, this vibration was no longer detected and an intense band was observed at 600 cm$^{-1}$. This frequency can be correlated with an Fe−O−Fe angle of 111°. This value suggests that the species which exists in these conditions is the protonated diamond core $[Fe(\mu\text{-}O)(\mu\text{-}OH)Fe]^{3+}$, analogous to that identified by Zang et al. (*J. Am. Chem. Soc.* **1994**, *116*, 3653) and by Hazell et al. (*J. Chem. Soc., Dalton Trans.* **1995**, 707). Upon addition of water, the original aquated species is observed in equilibrium with the protonated diamond unit. By analysis of the changes in UV−vis spectra as a function of the amount of water added, the equilibrium constant of the formation of the aquated species was found to be 5.4 M$^{-1}$.

### Introduction

Metalloproteins containing a nonheme diiron active site have been the subject of much interest in the past decade.[1−6] Some have been structurally characterized, such as the marine invertebrates' dioxygen carrier protein hemerythrin,[7] the hydroxylase component of methane monooxygenase (MMOH) from *Methylococcus capsulatus* (Bath)[8,9] and from *Methylosinus trichosporium*,[10] the R2 protein of the ribonucleotide reductase (RNR) from *Escherichia coli*,[11,12] and rubrerythrin from *De-*

[†] Université Paris-Sud.
[‡] Institut de Chimie des Substances Naturelles.
[§] Laboratoire de Chimie des Métaux de Transition, Univ. P. et M. Curie.
[||] Laboratoire de Chimie Structurale Organique et Biologique, Univ. P. et M. Curie.

(1) Wallar, B. J.; Lipscomb, J. D. *Chem. Rev.* **1996**, *96*, 2625−2657.
(2) Andersson, K. K.; Gräslund, A. *Adv. Inorg. Chem.* **1995**, *43*, 359−408.
(3) Stenkamp R. E. *Chem. Rev.* **1994**, *94*, 715−726.
(4) Feig, A. L.; Lippard, S. J. *Chem. Rev.* **1994**, *94*, 759−805.
(5) Vincent, J. B.; Olivier-Lilley, G. L.; Averill, B. A. *Chem. Rev.* **1990**, *90*, 1447−1467.
(6) Kurtz, D. M., Jr. *J. Biol. Inorg. Chem.* **1997**, *2*, 159−167.
(7) Holmes, M. A.; Le Trong, I.; Turley, L.; Sieker, L. C.; Stenkamp, R. E. *J. Mol. Biol.* **1991**, 218, 583.
(8) Rosenzweig, A. C.; Frederick, C. A.; Lippard, S. J.; Nordlund, P. *Nature* **1993**, *366*, 537−543.
(9) Rosenzweig, A. C.; Nordlund, P.; Takahara, P. M.; Frederick, C. A.; Lippard, S. J. *Chem. Biol.* **1995**, *2*, 409−418.
(10) Elango, N.; Radhakrishnan, R.; Froland, W. A.; Wallar, B. J.; Earhart, C. A.; Lipscomb, J. D.; Ohlendorf, D. H. *Protein Sci.* **1997**, *6*, 556−568.

S0020-1669(97)01589-9 CCC: $15.00 
Published on Web 06/09/1998

*sulfovibrio vulgaris*.[13] On the basis of spectroscopic data and supported by X-ray diffraction studies, purple acid phosphatases[5,14,15] and $\Delta^9$ stearoyl acyl carrier protein desaturase[16−18] also belong to this class of metalloproteins. No X-ray structure is available for the hydroxylase component of toluene-4-monooxygenase, altough it has been demonstrated that it contains a nonheme diiron site.[19]

In the deoxy form of hemerythrin, the two iron(II) ions are bridged by a hydroxo group and two carboxylato residues from aspartate and glutamate α-amino acids. After the fixation of dioxygen on one metal center, both iron ions are in the +3 oxidation state and bridged by an oxo group that is hydrogen bonded to the hydroperoxo terminal ligand.[3]

The X-ray diffraction work on rubrerythrin[13] allowed the determination of a ($\mu$-oxo)bis($\mu$-glutamato)diiron(III) core unit. The X-ray structure of $RNRR_{2ox}$ reveals that the two iron(III) centers are linked by an oxo group and a glutamate residue.[11] For $MMOH_{ox}$, the bridge also contains a carboxylato group from a glutamate amino acid and has either a $\mu$-hydroxo-$\mu$-acetato[8] connection or a diamond type core unit with a $\mu$-hydroxo-$\mu$-aquo[9] or a bis-$\mu$-hydroxo[10] double link.

The way dioxygen is activated by MMOH in order to perform the hydroxylation of methane to methanol has been the subject of many studies.[1] Several intermediates have been characterized. After the formation of an oxygen adduct (compound O), a peroxo intermediate named compound P is formed where the two iron centers are bridged by a peroxo group in a symmetric but not completely established mode ($\mu$-$\eta^2$,$\eta^2$ or $\mu$-1,2). It spontaneously converts to compound Q, and the Mössbauer data indicate an exchange-coupled high-valent $Fe^{IV}Fe^{IV}$ active site.[20] EXAFS experiments indicate a short Fe−Fe separation of 246 pm as well as a single 177 pm Fe−O bond per iron.[21] The authors have thus suggested the existence of an $Fe^{IV}{}_2O_2$ diamond core structure for compound Q that could be the key feature for oxidation of methane.

Progress has been made in the modeling of such enzymes. A number of $\mu$-oxo dinuclear Fe(III) complexes have been synthesized.[22,23] With tetradentate ligands of the tris(2-pyridylmethyl)amine (TPA) family, several complexes have been isolated. They have either a single $\mu$-oxo bridge,[24,25] or a double $\mu$-oxo-$\mu$-hydroxo[26] or bis-$\mu$-oxo[25] connection. By oxidation of $[TPA(H_2O)Fe(\mu\text{-}O)Fe(OH)TPA]^{3+}$, Dong et al. were able to isolate at low temperature an $[Fe(\mu\text{-}O)_2Fe]^{3+}$ entity[27] that was recently shown to hydroxylate C−H bonds.[28]

To isolate other dinuclear species containing the diamond core structure, we have explored the chemistry with *N*,*N*′-dimethyl-*N*,*N*′-bis(2-pyridylmethyl)ethane-1,2-diamine. Several di-iron(III) complexes with this ligand have already been isolated,[29−31] all containing the $[Fe(\mu\text{-}O)Fe]^{4+}$ motif with an extra bidentate molecule as a second bridge ($CO_3^{2-}$, $SO_4^{2-}$, $CH_3CO_2^-$). We report here the synthesis and the X-ray diffraction study of the mono-$\mu$-oxo bridging species $[L(H_2O)Fe(\mu\text{-}O)Fe(OH)L]^{3+}$ and its evolution in dry acetonitrile toward the protonated diamond form $[LFe(\mu\text{-}O)(\mu\text{-}OH)FeL]^{3+}$. Addition of water displaces the equilibrium toward the $[L(H_2O)Fe(\mu\text{-}O)Fe(OH)L]^{3+}$ form. The importance of elimination of water to stabilize the diamond form is thus demonstrated.

## Experimental Section

**Compound Preparation.** Reagents and solvents were purchased commercially and used as received. Acetonitrile used for solution studies was distilled before use and dried on an alumina column.

***Caution!*** *Perchlorate salts of metal complexes with organic ligands are potentially explosive. Only small quantities of these compounds should be prepared and handled behind suitable protective shields.*

***N*,*N*′-Dimethyl-*N*,*N*′-bis(2-pyridylmethyl)ethane-1,2-diamine (L).** This ligand was prepared by a method which was a slight modification of the synthetic route proposed by Toftlund.[32] To a 20 mL aqueous solution of *N*,*N*′-dimethylethane-1,2-diamine (0.88 g, 10 mmol) was added 2 equiv of 2-picolyl chloride in hydrochloride form dissolved in 20 mL of water. After mixing, 4 equiv of sodium hydroxide were added. After refluxing for 1 h at 70 °C, the organic phase is extracted with toluene, dried on $Na_2SO_4$, and concentrated under vacuum. The ligand L is obtained as a yellow oil (84% yield). $^1$H NMR ($CDCl_3$): $\delta$ (ppm) 2.3 (s, 3H, $-CH_3$), 2.65 (s, 2H, $-CH_2-CH_2-$N), 3.7 (s, 2H, py$-CH_2-$N), 7.1 (m, 1H), 7.4 (d, 1H), 7.6 (m, 1H), 8.5 (d, 1H).

**$[L(H_2O)Fe(\mu\text{-}O)Fe(OH)L](ClO_4)_3\cdot H_2O$ (1).** Compound **1** was prepared by mixing under an argon atmosphere 10 mL of deoxygenated ethanol/water 1:1 solution containing L (0.8 mmol) and sodium hydroxide (1 mmol) with 2 mL of a deoxygenated ethanol solution of $Fe(ClO_4)_3\cdot 6H_2O$ (1 mmol). The red-brownish solution was allowed to slowly evaporate under a small argon gas current. Green crystals formed after 2 days. Anal. Calcd for $[L(H_2O)Fe(\mu\text{-}O)Fe(OH)L](ClO_4)_3\cdot H_2O$ ($C_{32}H_{49}Cl_3Fe_2N_8O_{16}$): C, 37.69; H, 4.84; Cl, 10.43; N, 10.99. Found: C, 37.01; H, 4.69; Cl, 10.25; N, 10.84.

**Crystallographic Studies. Complex 1.** A yellow-grey prism single crystal of 0.20 × 0.40 × 0.90 mm was mounted on an Enraf-Nonius CAD4 diffractometer with graphite-monochromated Mo Kα radiation ($\lambda$ = 0.7107 Å). The unit cell dimensions were obtained from the least-squares refinement of the setting angles of 25 reflections [7.8° < Θ < 9.5°]. The data collection was made at room temperature, with Θ−2Θ scan technique mode in the Θ range from 2 to 30°. Three standard reflections were measured every 3 h to monitor instrument and crystal stability. No significant decay was observed.

(11) Nordlund, P.; Sjöberg, B.-M.; Eklund H. *Nature* **1990**, *345*, 593−598.
(12) Nordlund, P.; Eklund, H. *J. Mol. Biol.* **1993**, *232*, 123−164.
(13) deMaré, F.; Kurtz, D. M., Jr.; Nordlund, P. *Nat. Struct. Biol.* **1996**, *3*, 539−546.
(14) True, A. E.; Scarrow, R. C.; Randall, C. R.; Holz, R. C.; Que, L., Jr. *J. Am. Chem. Soc.* **1993**, *115*, 4246−4255.
(15) (a) Sträter, N.; Klabunde, T.; Tucker, P.; Witzel, H.; Krebs, B. *Science*, **1995**, *268*, 1489−1492. (b) Klabunde, T.; Sträter, N.; Krebs, B.; Witzel, H. *FEBS Lett.* **1995**, *367*, 56−60.
(16) Fox, B. G.; Shanklin, J.; Somerville, C.; Münck, E. *Proc. Natl. Acad. Sci. U.S.A.* **1993**, *90*, 2486-2490.
(17) Fox, B. G.; Shanklin, J.; Ai, J.; Loehr, T. M.; Sanders-Loehr, J. *Biochemistry* **1994**, *33*, 12776−12786.
(18) Lindqvist, Y.; Huang, W.; Schneider, G.; Shanklin, J. *EMBO J.* **1996**, *15*, 4081−4092.
(19) Pikus, J. D.; Studts, J. M.; Achim, C.; Kauffmann, K. E.; Münck, E.; Steffan, R. J.; McClay, K.; Fox, B. G. *Biochemistry* **1996**, *35*, 9106−9119.
(20) Lee, S.-K.; Fox, B. G.; Froland, W. A.; Lipscomb, J. D.; Münck, E. *J. Am. Chem. Soc.* **1993**, *115*, 6450−6451.
(21) Shu, L.; Nesheim, J. C.; Kauffmann, K.; Münck, E.; Lipscomb, J. D.; Que, L., Jr. *Science* **1997**, *275*, 515−518.
(22) Kurtz, D. M., Jr. *Chem. Rev.* **1990**, *90*, 585−606.
(23) Weihe, H.; Güdel, H. U. *J. Am. Chem. Soc.* **1997**, *119*, 6539−6543 and references therein.
(24) Hazell, A.; Jensen, K. B.; MacKenzie, C. J.; Toftlund, H. *Inorg. Chem.* **1994**, *33*, 3127−3134.
(25) Zang, Y.; Dong, Y.; Que., L., Jr; Kauffmann, K.; Münck, E. *J. Am. Chem. Soc.* **1995**, *117*, 1169−1170.
(26) Zang, Y.; Pan, G.; Que, L., Jr.; Fox, B. G.; Münck, E. *J. Am. Chem. Soc.* **1994**, *116*, 3653−3654.
(27) Dong, Y.; Fujii, H.; Hendrich, M. P.; Leising, R. A.; Pan, G.; Randall, C. R.; Wilkinson, E. C.; Zang, Y.; Que, L., Jr.; Fox, B. G.; Kauffmann, K.; Münck, E. *J. Am. Chem. Soc.* **1995**, *117*, 2778−2792.
(28) Kim, C.; Dong, Y.; Que, L., Jr. *J. Am. Chem. Soc.* **1997**, *119*, 3635−3636.
(29) Arulsamy, N.; Goodson, P. A.; Hodgson, D. J.; Glerup, J.; Michelsen, K. *Inorg. Chim. Acta* **1994**, *216*, 21−29.
(30) Hazell, R.; Jensen, K. B.; MacKenzie, C. J.; Toftlund, H. *J. Chem. Soc., Dalton Trans.* **1995**, 707−717.
(31) Okuno, T.; Ito, S.; Ohba, S.; Nishida, Y. *J. Chem. Soc., Dalton Trans.* **1997**, 3547−3551.
(32) Toftlund, H.; Pedersen, E.; Yde-Andersen, S. *Acta Chem. Scand., Ser. A* **1984**, *38*, 693−697.

**Table 1.** Crystallographic Data for Complex **1**

| | |
|---|---|
| empirical formula | $C_{32}H_{49}N_8O_{16}Cl_3Fe_2$ |
| fw | 1019.84 |
| temperature (K) | 294(2) |
| wavelength (Å) | Mo Kα, 0.710 70 |
| space group | $P2_12_12_1$ |
| *a* (Å) | 13.283(5) |
| *b* (Å) | 16.050(9) |
| *c* (Å) | 20.050(9) |
| α (deg) | 90 |
| *β* (deg) | 90 |
| *γ* (deg) | 90 |
| *V* (Å$^3$) | 4476(6) |
| Z | 4 |
| $D_{calc}$ (g cm$^{-3}$) | 1.513 |
| $\mu$ (cm$^{-1}$) | 9.02 |
| $R(F^2)$ [$I > 2\sigma(I)$][a] | R1 = 0.0566, wR2 = 0.1414 |
| *R* indices for all data[a] | R1 = 0.1475, wR2 = 0.1842 |

[a] $R1 = \sum||F_o| - |F_c||/\sum|F_o|$; $wR2 = \{\sum[w(F_o^2 - F_c^2)^2]/\sum[w(F_o^2)^2]\}^{1/2}$.

A total of 6900 reflections were collected [$0 \le h \le 18$, $0 \le k \le 22$, $0 \le l \le 28$]. From 5638 unique reflections, 3783 were used ($I > 2\sigma(I)$). These data were corrected for Lorentz and polarization factors. An empirical absorption correction was applied using the program XABS2.[33]

The structure was solved by direct methods with the program SHELXS86[34] and refined on $F^2$ for all reflections by least-squares method using SHELXL-93.[35] All hydrogen atoms were located on difference Fourier syntheses, except one of a water molecule solvent, included in the crystal structure. Hydrogen atoms were included in the refinement at their ideal positions ($C-H_{ar} = 0.93$ Å, $C-H_{Me} = 0.96$ Å) and assigned an isotropic thermal parameter of 1.2 that of the bonded atoms, whereas the hydrogen atoms of the hydroxyl group and water molecules, located from the $\Delta\rho$ were fixed during the subsequent calculations. One of the three perchlorate counterions is affected by disorder. Two positions were found on the difference Fourier syntheses. Better convergence was obtained with occupancies of 0.8 and 0.2 for the ion, and refinement was pursued with restraints. The final conventional *R* factor is 0.056 for 3783 ($F_o > 4\sigma(F_o)$) and 588 parameters and 0.1375 for all data, $wR(F^2) = 0.18$ for all, $w = 1/[\sigma^2(F_o)^2 + (0.0895P)^2 + 2.2313P]$ where $P = (F_o^2 + 2F_c^2)/3$. The largest difference peak and hole are 0.60 and 0.48 e Å$^{-3}$, respectively. Crystal data are summarized in Table 1.

**Electrospray Ionization Mass Spectroscopy (ESI-MS).** ESI-MS measurements were performed using a modified NERMAG R10-10 quadrupole mass spectrometer, equipped with an Analytica of Brandford electrospray source (Quad Service, Poissy, France). The range of the instrument was 10−2000 *m*/*z*. The spectra were recorded over the 50−2000 *m*/*z* range, in steps of 1 *m*/*z*. The output signal of the electron multiplier was transferred to a PC for treatment of the spectra. The MST mass treatment program was developed in the Laboratoire of Chimie Structurale Organique et Biologique[36] according to the algorithm of Reinhold et al.[37] The complex was analyzed in the positive mode after dilution at approximatively $10^{-4}$ M in dry acetonitrile. The entry capillary voltage used was −2700 V. The sample was infused into the source using a Harvard 11 syringe pump at a flow rate of 2 μL min$^{-1}$. The exit capillary voltage was 60 V, and the first skimmer voltage was 50 V. The $N_2$ temperature was 75 °C with a pressure of $68.95 \times 10^3$ Pa at 5 L min$^{-1}$.

**Raman Spectroscopy.** Raman spectra were recorded on a Jobin-Yvon $U_{1000}$ double monochromator equipped with an As Ga photomultiplier and photocounting detection. The excitation wavelength line was the 413.1 nm line of a $Kr^+$ laser at 10−15 mW incident power level. Solid sample of complex **1** was mounted on a disk rotating at about 1000 rpm. The spectral width was 4 cm$^{-1}$. Solution samples were transferred in a degassed rotating cell. The spectral resolution was 6 cm$^{-1}$.

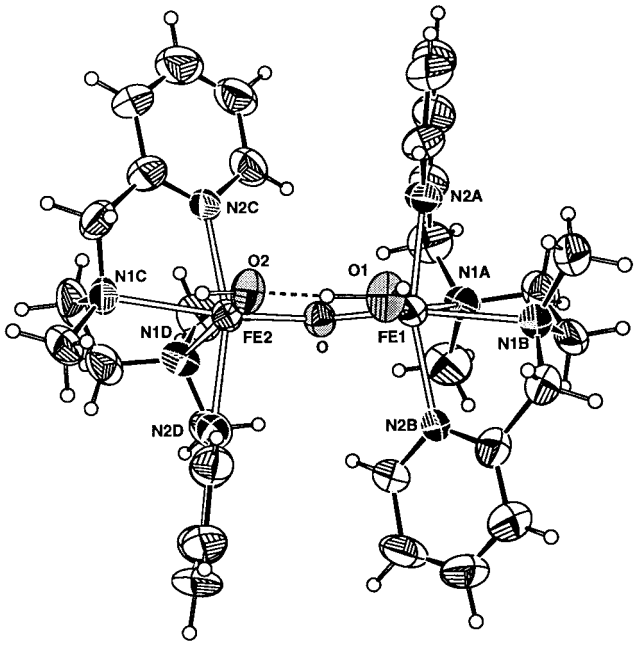


**Figure 1.** ORTEP view of the $[L(H_2O)Fe(\mu\text{-}O)Fe(OH)L]^{3+}$ cation in the crystal of complex **1**, showing the 50% probability thermal ellipsoids.

**Table 2.** Selected Bond Lengths (Å) and Angle (deg) for **1**

| | |
|---|---|
| Fe(1)···Fe(2) | 3.396(1) |
| Fe(1)−O | 1.817(4) |
| Fe(1)−O(1) | 2.046(4) |
| Fe(1)−N(2A) | 2.147(6) |
| Fe(1)−N(2B) | 2.163(6) |
| Fe(1)−N(1A) | 2.264(6) |
| Fe(1)−N(1B) | 2.322(6) |
| Fe(2)−O | 1.827(4) |
| Fe(2)−O(2) | 1.990(4) |
| Fe(2)−N(2D) | 2.160(6) |
| Fe(2)−N(2C) | 2.180(6) |
| Fe(2)−N(1D) | 2.291(6) |
| Fe(2)−N(1C) | 2.320(6) |
| Fe(1)−O−Fe(2) | 137.5(2) |

**Magnetic Susceptibility Measurements.** Magnetic susceptibility data were recorded on a MPMS5 magnetometer (Quantum Design Inc.). The calibration was made at 298 K using a palladium reference sample furnished by Quantum Design Inc. The data were collected over a temperature range of 10−300 K at a magnetic field of 1.0 T and were corrected for diamagnetism.

**EPR Spectroscopy.** EPR spectra were recorded on Bruker ER 200 D and 300 spectrometers at X-band. For low-temperature studies, an Oxford Instrument continuous flow liquid helium cryostat and a temperature control system were used.

## Results and Discussion

**X-ray Crystal Structure of $[L(H_2O)Fe(\mu\text{-}O)Fe(OH)L](ClO_4)_3\cdot H_2O$ (1).** The asymmetric unit consists of one $[L(H_2O)Fe(\mu\text{-}O)Fe(OH)L]^{3+}$ complex cation, three perchlorate anions, and one water solvent molecule. An ORTEP representation of the cation is presented in Figure 1, and a selection of bond lengths and angles is in Table 2. The iron atoms, Fe1 and Fe2, separated by 3.396(1) Å, are linked by an oxo ion. The two

(33) Parkin, S.; Moezzi, B.; Hope, H. *J. Appl. Crystallogr.* **1995**, *28*, 53−56.
(34) Sheldrick, G. M. *Acta Crystallogr., Sect. A* **1990**, *46*, 467.
(35) Sheldrick, G. M. *SHELXL-93: Program for the refinement of crystal structures*; University of Göttingen: Germany, 1993.
(36) Blasco, T.; Luvan, M. XIIIth JFSM, Orléans, 17−19 September 1996, I57.
(37) Reinhold: B. B.; Reinhold, V. N. *J. Am. Soc. Mass Spectrom.* **1992**, *3*, 207.

**Table 3.** Main Characteristics of the $[(H_2O)Fe(\mu\text{-}O)Fe(OH)]^{3+}$ Core Unit[a]

| | TPA | 5-$Et_3$-TPA | bispic$Me_2$en |
|---|---|---|---|
| Fe1−($\mu$-O) | 1.780(6) | 1.779(5) | 1.817(4) |
| Fe2−($\mu$-O) | 1.839(6) | 1.826(5) | 1.827(4) |
| Fe1−O1($OH_2$) | 2.040(9) | 2.049(6) | 2.046(4) |
| Fe2−O2(OH) | 1.913(7) | 1.907(7) | 1.990(4) |
| Fe1···Fe2 | 3.389(2) | 3.346(9) | 3.396(1) |
| O1···O2 ($H_3O_2^-$) | 2.419(10) | 2.464(9) | 2.450(7) |
| Fe1−($\mu$-O)−Fe2 | 138.9(4) | 136.3(3) | 137.5(2) |
| Fe1−O1···O2−Fe2 | 24.0(5) | 20.5(9) | 6.6(4) |

[a] Distances are given in angstroms, and angles, in degrees.

Fe($\mu$-O) lengths are 1.817(4) and 1.827(4) Å. The Fe−($\mu$-O)−Fe angle is 137.5(2)°. The ligand L is coordinated to the iron centers by the pyridine nitrogen atoms in axial position and the two nitrogen amine atoms in equatorial ligation providing the cis-α conformation. The sixth coordination site is occupied by a water molecule on the Fe1 and an hydroxyl group on the Fe2. The assignment has been possible based on the location of the three hydrogen atoms of the $H_3O_2^-$ bridge. The Fe1−O1 distance is 2.046(4) Å and the Fe2−O2 bond length is 1.990(4) Å. The water and hydroxyl oxygen atoms O1 and O2, located cis to each other are linked by a strong linear intramolecular hydrogen bond as indicated by the 2.450(7) Å O1···O2 separation with the O1−H2···O2 angle of 159°. The H-bond network is completed by four intermolecular H bonds involving both oxygen atoms of the hydroxyl and water ligands, and at the same time the three perchlorate anions and the water solvent molecule included in the crystal structure. The main features of the three-dimensional H-bond scheme are reported in Figure S1 and are listed in Table S6 of the Supporting Information.

The coordination of the ligand L is comparable to that found in other complexes with the same ligand[29−31] or its monomethyl derivative, *N*-methyl-*N*,*N*′-bis(2-pyridylmethyl)ethane-1,2-diamine.[38]

The $[(H_2O)Fe(\mu\text{-}O)Fe(OH)]^{3+}$ core unit presents some differences with the other two previously published structures (TPA,[24] 5-$Et_3$-TPA[27]). The main features of the three core structures are collected in Table 3. It clearly shows the higher symmetry found here. The Fe1-($\mu$-O) and Fe2-($\mu$-O) distances are much closer to each other than in the other two dimers. The same holds for the Fe1−O1 and Fe2−O2 distances, although the value for the former is quite reminiscent of that of an Fe(III)−aquo bond. A relevant structural feature could be the remarkable conformation of the ($\mu$-O)($\mu$-$H_3O_2$) diiron core, the four atoms Fe1, Fe2, O1, and O2 being in the same plane, in contrast to what was found in the other two structures.

**Magnetic Susceptibility Measurements.** The molar magnetic susceptibility $\chi_M$ of a powder sample of $[L(H_2O)Fe(\mu\text{-}O)Fe(OH)L](ClO_4)_3\cdot H_2O$ was measured as a function of the temperature *T*. $\chi_M T$ decreases from 0.96 $cm^3\ mol^{-1}$ K at 300 K to a 0 plateau below 40 K. This is characteristic of an antiferromagnetic interaction between the electronic spins of the $Fe^{III}$ ions which produces a spin $S = 0$ diamagnetic ground state. The susceptibility was calculated as

$$\chi_M = \frac{N\mu_B^2 g^2}{3kT} \quad \frac{\sum S(S+1)(2S+1)\exp\left(\frac{JS(S+1)}{2kT}\right)}{\sum (2S+1)\exp\left(\frac{JS(S+1)}{2kT}\right)}$$

The best fit was obtained for $J = -184\ cm^{-1}$ by setting $g = 2$. This is in agreement with the previously published values for $[(TPA)(H_2O)Fe(\mu\text{-}O)Fe(OH)(TPA)]^{3+}$ ($J = -196\ cm^{-1}$)[24] and $[(5\text{-}Et_3\text{-}TPA)(H_2O)Fe(\mu\text{-}O)Fe(OH)(5\text{-}Et_3\text{-}TPA)]^{3+}$ ($J = -194\ cm^{-1}$).[27]

**Raman Spectra.** In the solid state, the Raman spectrum of compound **1** presents a band at 438 $cm^{-1}$ that was assigned to the symmetric stretching vibration of the Fe−O−Fe core.[27,39] From the correlation published by Sanders-Loehr et al.,[39] the 137.5° Fe−($\mu$-O)−Fe angle value determined by X-ray diffraction would lead to a 485 $cm^{-1}$ wavenumber. It must be noted that the compounds on which the correlation has been made exhibit Fe−($\mu$-O) distances shorter than the 1.822 Å average bond length observed here. One can expect that such a bond lengthening would be accompanied by a decrease in the stretching frequency.

**Equilibrium between $[L(H_2O)Fe(\mu\text{-}O)Fe(OH)L]^{3+}$ and $[LFe(\mu\text{-}O)(\mu\text{-}OH)FeL]^{3+}$ in Acetonitrile in the Presence of Water. Raman spectra.** A Raman spectrum was recorded immediately after dissolution of compound **1** in acetonitrile under argon. It is reproduced in Figure 2 (spectrum a). The band observed at 438 $cm^{-1}$ in the solid state is now very weak and shifted to 444 $cm^{-1}$ while an intense band at 600 $cm^{-1}$ with a shoulder at 581 $cm^{-1}$ appears. Hazell et al.[30] have observed a band at 593 $cm^{-1}$ and attributed it to the double-bridged $[LFe(\mu\text{-}O)(\mu\text{-}OH)FeL]^{3+}$ species. In $[(6\text{-}Me_3\text{-}TPA)Fe(\mu\text{-}O)(\mu\text{-}OH)Fe(6\text{-}Me_3\text{-}TPA)]^{3+}$, the Fe−O−Fe angle is equal to 98.7° and the symmetric vibration is detected at 676 $cm^{-1}$.[40] It thus appears that upon dissolution in $CH_3CN$, the aqua ligand is lost and the terminal hydroxo group becomes a bridging ligand leading to the formation of the double-bridged $[LFe(\mu\text{-}O)(\mu\text{-}OH)FeL]^{3+}$ species.

$^{18}O$-labeled water was added to check the possible reversibility of this conversion. For a 99:1 v:v $CH_3CN/H_2O$ solvent composition, the Raman spectrum changes dramatically (spectrum b of Figure 2). The intensity of the symmetric stretching vibration observed at 600 $cm^{-1}$ decreases, and the band at 444 $cm^{-1}$ increases. Such a frequency is expected for an Fe−O−Fe angle of 141.5° and indeed is the signature of the $[L(H_2O)Fe(\mu\text{-}O)Fe(OH)L]^{3+}$ species. This thus proves that the following equilibrium exists:

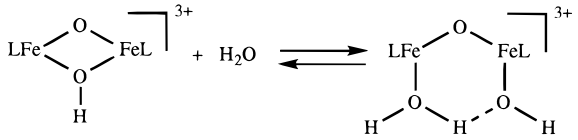


A quantitative analysis of this equilibrium is presented below. The same behavior was observed when normal water is added to the medium (data not shown). No $^{18}O$ shift was detected which can be interpreted as a slow exchange of the $\mu$-oxo bridge in both complexes.

**ESI-MS Spectrum.** The ESI-MS spectrum was also recorded immediately after dissolution of complex **1** in acetonitrile. The peaks detected for *m*/*z* values higher than 300 *m*/*z* can be fully interpreted as monopositively charged species as indicated in Figure 3. It is consistent with the assumption formulated above in the Raman spectroscopy analysis, that is, the spontaneous formation of the $\mu$-oxo-$\mu$-hydroxo cation upon dissolution in acetonitrile. Note that no species containing a

(38) Nivorozhkin, A. L.; Anxolabéhère-Mallart, E.; Mialane, P.; Davidov, R.; Guilhem, J.; Césario, M.; Audière, J.-P.; Girerd, J.-J.; Styring, S.; Schussler, L.; Seris, J.-L. *Inorg. Chem.* **1997**, *36*, 846−853.

(39) Sanders-Loehr, J.; Weehler, W. D.; Shiemke, A. K.; Averill, B. A.; Loehr, T. M. *J. Am. Chem. Soc.* **1989**, *111*, 8084−8093.

(40) Wilkinson, E. C.; Dong, Y.; Zang, Y.; Fujii, H.; Fraczkiewicz, R.; Fraczkiewicz, G.; Czernuszewicz, R. S.; Que, L., Jr. *J. Am. Chem. Soc.* **1998**, *120*, 955−962, footnote 13.

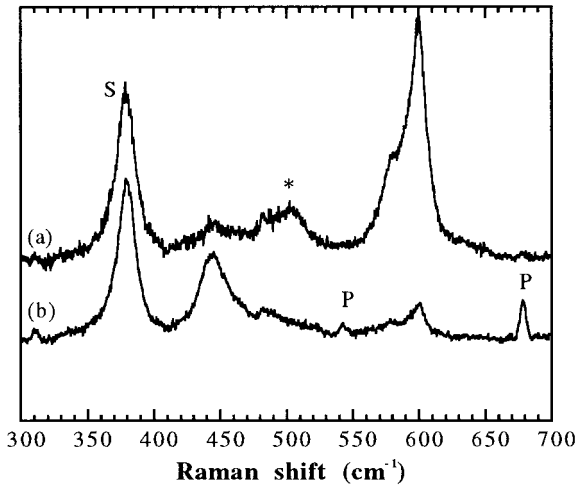


**Figure 2.** Raman spectra of compound **1** (a) immediately after dissolution in acetonitrile and (b) with 1% $^{18}OH_2$ added. S and P respectively designate solvent and plasma lines. The band marked with an asterisk (*) corresponds to a cell contribution.

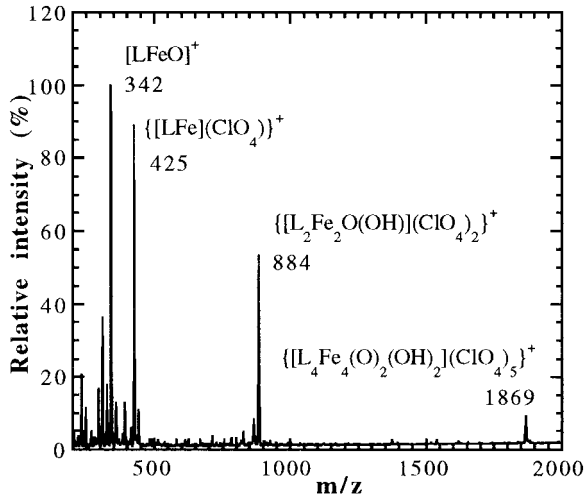


**Figure 3.** ESI-MS spectrum of a freshly prepared dry acetonitrile solution of complex **1**.

coordinated water or acetonitrile molecule have been detected under these soft conditions, with a low difference of 10 V between the capillary exit and the first skimmer voltages.

**UV−Visible Spectra.** In Figure 4 is reported the spectrum a obtained for a freshly prepared solution of **1**. In fact, it is close to the one published for $[LFe(\mu\text{-}O)(\mu\text{-}OH)FeL]^{3+}$.[30] Table 4 collects wavelengths and absorption coefficients.

The 550−700 nm region has been reported to be a signature of the Fe−O−Fe unit which strongly depends on the bridge angle:[41] the more energetic, the less bent. An other signature of this core presenting the same behavior is detected between 400 and 550 nm, the intensity of which increases as the Fe−($\mu$-O)−Fe angle decreases. As previously mentioned by Hazell et al.,[30] the 555 nm band observed for **1** is associated with a significant red shift which is correlated with a closing of the Fe−($\mu$-O)−Fe angle. When one makes a linear graph of $\lambda_{max}$ as a function of the bridging angle (Table VII of ref 41), 555 nm would correspond to 111°. Again, this is in favor of the formation of the $[Fe(\mu\text{-}O)(\mu\text{-}OH)Fe]^{3+}$ core unit. Note that for the cation $[(6\text{-}Me_3\text{-}TPA)Fe(\mu\text{-}O)(\mu\text{-}OH)Fe(6\text{-}Me_3\text{-}TPA)]^{3+}$, Zang et al.[26] reported a band at similar wavelength ($\lambda$ = 550 nm)

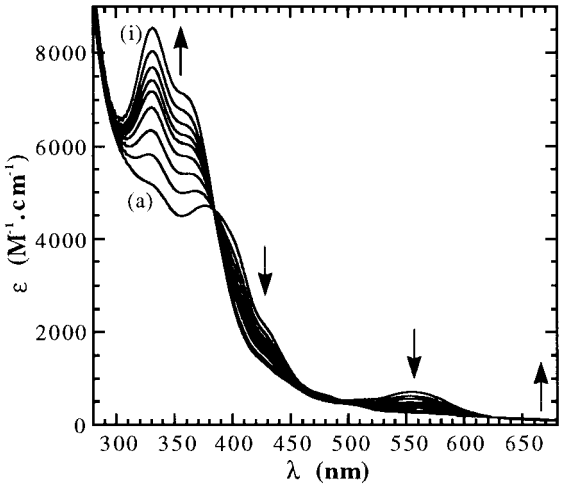


**Figure 4.** Evolution of the UV−visible spectrum of compound **1** dissolved in dry acetonitrile upon addition of water. Spectrum a is recorded on the freshly prepared solution ($5.44 \times 10^{-7}$ mol of **1** in 3 mL) and corresponds to $[L(Fe(\mu\text{-}O)(\mu\text{-}OH)FeL]^{3+}$. Spectra b−h correspond respectively to $1.33 \times 10^{-4}$, $2.94 \times 10^{-4}$, $5.54 \times 10^{-4}$, $8.31 \times 10^{-4}$, $11.08 \times 10^{-4}$, $16.62 \times 10^{-4}$, and $33.25 \times 10^{-4}$ mol of water added to the cell. Spectrum i of the $[L(H_2O)Fe(\mu\text{-}O)Fe(OH)L]^{3+}$ cation is calculated (see text).

**Table 4.** Wavelengths and Molecular Absorption Coefficients ($\epsilon$ in $M^{-1}$ $cm^{-1}$) for Compound **1** in Acetonitrile

| $[LFe(\mu\text{-}O)(\mu\text{-}OH)FeL]^{3+}$ | | $[L(H_2O)Fe(\mu\text{-}O)Fe(OH)L]^{3+}$ | |
|---|---|---|---|
| $\lambda_{max}$ (nm) | $\epsilon$ ($M^{-1}$ cm−1) | $\lambda_{max}$ (nm) | $\epsilon$ ($M^{-1}$ $cm^{-1}$) |
| 377 | 4714 | 332 | 8523 |
| 430 | 2072 (sh) | 360 | 7080 |
| 479 | 650 | 430 | 1282 |
| 512 | 540 | 479 | 524 |
| 555 | 702 | 512 | 396 |
| | | 555 | 255 |

with a molar absorption coefficient of the same magnitude ($\epsilon$ = 670 $M^{-1}$ $cm^{-1}$).

When water is added to the medium, spectra b−h of Figure 4 are recorded. The 555 nm band and those observed at 377 and 430 nm decrease in intensity as water is added to the solution, suggesting the disappearance of this double-bridged system in favor of a mono-$\mu$-oxo cluster as mentioned earlier.[30] Three isosbestic points are seen at 385, 624, and 712 nm (not shown) suggesting an equilibrium between two species. Previously reported UV−visible spectra of other $[(H_2O)Fe(\mu\text{-}O)Fe(OH)]^{3+}$ clusters synthesized with TPA or 5-$Et_3$-TPA present a band at 605 or 608 nm of lower intensity ($\epsilon \approx 160$ or 165 $M^{-1}$ $cm^{-1}$), consistent with a 140° Fe−O−Fe angle, suggesting the persistence in solution of the $H_3O_2^-$ bridge. This band is detected around 650 nm only after addition of a great amount of water (6000 equiv, spectrum h). The $^6A_1 \rightarrow (^4E, {}^4A_1)$ transition, which is independent of the Fe−O−Fe angle, occurs around 490 nm. The fact that the 460−520 nm region of the spectrum remains unchanged upon addition of water indicates that the oxo bridge is maintained, which is indeed confirmed by EPR studies: no signal is detected at helium temperature. The bands at 330 and 365 nm are due to ligand-to-metal charge-transfer transitions.

**Quantitative Analysis of the Equilibrium.** We saw above that upon addition of water, the hydroxo bridge is broken, leaving a free coordination site for the fixation of a water molecule on one iron. The fact that the evolution of the UV−visible spectrum is observed upon addition of 200−6000 equiv of water with the persistence of the isosbestic points strongly

(41) Norman, R. E.; Holz, R. C.; Ménage, S.; O'Connor, C. J.; Zhang, J. H.; Que, L., Jr. *Inorg. Chem.* **1990**, *29*, 4629−4637.

suggests that the equilibrium is difficult to shift completely to the right. A quantitative analysis of the UV−visible spectra was done to determine

$$K = \frac{|[L(HO)Fe(\mu\text{-}O)Fe(OH_2)L]^{3+}|}{|[LFe(\mu\text{-}O)(\mu\text{-}OH)FeL]^{3+}|\ |H_2O|}$$

We assume that only the two cations $[LFe(\mu\text{-}O)(\mu\text{-}OH)FeL]^{3+}$ and $[L(HO)Fe(\mu\text{-}O)Fe(OH_2)L]^{3+}$ contribute to the optical density observed. Thus, the molecular fractions depend only on the product $K \times |H_2O|$ where $|H_2O|$ stands for the concentration of free water. Since the first addition brings 100 equiv of water, we approximate $|H_2O|$ to the amount of the water added divided by the volume of the solution studied neglecting the dilution.

Experimental spectra b−h can be perfectly reproduced as the combination in variable amounts of the experimental spectrum a of the double-bridged complex and of the calculated spectrum i of the single-bridged complex, this procedure allowing the determination of $K = 5.4$ L mol$^{-1}$. This value is in agreement with the fact that upon dissolution in $CH_3CN$ the transformation of complex **1** is quantitative since in those conditions only two water molecules per dinuclear unit are introduced. This is indeed not enough to displace the equilibrium toward the mono-oxo-bridged species. If the effect of water on $[LFe(\mu\text{-}O)(\mu\text{-}OH)FeL]^{3+}$ has been reported previously, the equilibrium has not been quantitatively studied.[30] This reaction does not seem to occur when TPA or 5-Et$_3$-TPA is used.

The formation of the $\mu$-oxo-$\mu$-hydroxo core unit upon dissolution of **1** in $CH_3CN$ is similar to the second step of the mechanism suggested for the formation of the double-hydroxo-bridged dimeric species starting from a cis-hydroxoaquo monomeric complex.[42] It has been proposed that the activation barrier decreases as the torsional M−O···O−M angle decreases.[42] This remark could explain why the elimination of water in **1** was easily observed.

As for the reverse reaction, it has already been reported for a di-$\mu$-hydroxo dichromium(III) complex with an equilibrium constant $[(H_2O)M(\mu\text{-}OH)M(OH)]^{4+}/[M(\mu\text{-}OH)_2M]^{4+} = 0.83$ measured in water.[43] Although it is not straightforward to compare this value to ours due to the difference in solvents, the very fact that this equilibrium could be observed in water for chromium(III) indicates that the open form is less stable for chromium(III) than for iron(III).

## Conclusion

The third example of the hydrogen-bonded $[(H_2O)Fe(\mu\text{-}O)Fe(OH)]^{3+}$ core was identified with the terminal tetradentate ligand *N*,*N*′-dimethyl-*N*,*N*′-bis(2-pyridylmethyl)ethane-1,2-diamine. Its structure reveals a planar conformation of the hydrogen-bonded motif. The spontaneous substitution of the coordinated water molecule in $[(H_2O)Fe(\mu\text{-}O)Fe(OH)]^{3+}$ by the hydroxo group leading to an $[Fe(\mu\text{-}O)(\mu\text{-}OH)Fe]^{3+}$ core unit was detected by UV−vis and Raman spectroscopies on a solution of compound **1** in dry acetonitrile. When water was added to the dry acetonitrile solution, Raman and UV−visible data clearly indicated the breaking of the hydroxo link and the back-formation of the $[L(H_2O)Fe(\mu\text{-}O)Fe(OH)L]^{3+}$ cation. In presence of water both species coexist, and in an anhydrous enough medium it is possible to isolate the protonated diamond core. These observations could help in the investigations of high oxidation states of the diamond core by electrochemical oxidation. This problem is currently under study.

The protonated form of the diamond core $[Fe(\mu\text{-}O)(\mu\text{-}OH)Fe]^{3+}$ is thus sensitive to the presence of water. We speculate that the diamond core $[Fe(\mu\text{-}OH)_2Fe]^{3+}$ [10] in MMO is stabilized due to the hydrophobicity of the active site. The restricted accessibility of water to the iron site in MMO has been illustrated by the slow H/D exchange rate found by ENDOR and pulsed EPR experiments.[44,45] This argument is still more appropriate to account for the stability of the $[Fe^{IV}O_2Fe^{IV}]^{4+}$ active species of MMO which ought to be more sensitive to hydrolysis.

**Acknowledgment.** We thank Pr. J.-C. Tabet for stimulating discussions.

**Supporting Information Available:** Listings of complete information on collection data and refinement of the structure, complete atomic coordinates, bond lengths and angles, and anisotropic thermal parameters of non-hydrogen atoms, anisotropic displacement parameters, and hydrogen atom coordinates for **1** (Tables S1−S5); the main features of the three-dimensional H-bond scheme are reported in Figure S1 and listed in Table S6 (12 pages). Ordering information is given on any current masthead page.

IC971589E

(42) Ardon, M.; Bino, A.; Michelsen, K. *J. Am. Chem. Soc.* **1987**, *109*, 1986−1990 and references therein.
(43) Springborg, J.; Toftlund, H. *J. Chem. Soc., Chem. Commun.* **1975**, 422−423 and references therein.
(44) DeRose, V. J.; Liu, K. E.; Kurtz, D. M., Jr.; Hoffman, B. M.; Lippard, S. J. *J. Am. Chem. Soc.* **1993**, *115*, 6440−6441.
(45) Thomann, H.; Bernardo, M.; McCormick, J. M.; Pulver, S.; Andersson, K. K.; Lipscomb, J. D.; Solomon, E. I. *J. Am. Chem. Soc.* **1993**, *115*, 8881−8882.